

# Synthesis, structure, DNA-binding properties and antioxidant activity of a nickel(II) complex with bis(*N*-allylbenzimidazol-2-ylmethyl)benzylamine

Huilu Wu\*, Jingkun Yuan, Ying Bai, Guolong Pan, Hua Wang, Xingbin Shu

School of Chemical and Biological Engineering, Lanzhou Jiaotong University, Lanzhou 730070, PR China

## ARTICLE INFO

### Article history:

Received 9 November 2011  
Received in revised form 23 November 2011  
Accepted 30 November 2011  
Available online 21 December 2011

### Keywords:

Benzimidazole  
Nickel(II) complex  
Crystal structure  
DNA-binding property  
Antioxidant property

## ABSTRACT

A V-shape ligand bis(*N*-allylbenzimidazol-2-ylmethyl)benzylamine (babb) and its nickel complex, [Ni(babb)<sub>2</sub>](pic)<sub>2</sub> (pic = picrate), have been synthesized and characterized by physico-chemical and spectroscopic methods. Single-crystal X-ray revealed that the coordination sphere around Ni(II) is distorted octahedral with a N<sub>6</sub> ligand set, in which six nitrogen atoms were afforded by two tridentate ligand babb. The DNA-binding properties of the free ligand babb and Ni(II) complex have been investigated by electronic absorption, fluorescence, and viscosity measurements. The results suggest that babb and Ni(II) complex both bind to DNA via an intercalative binding mode, and the affinity for DNA is more strong in case of Ni(II) complex when compared with babb. The intrinsic binding constants (*K*<sub>b</sub>) of the Ni(II) complex and ligand with DNA were  $3.65 \times 10^4 \text{ M}^{-1}$  and  $2.26 \times 10^3 \text{ M}^{-1}$ , respectively. Additionally, Ni(II) complex also exhibited potential antioxidant properties *in vitro* studies.

© 2011 Elsevier B.V. All rights reserved.

## 1. Introduction

The benzimidazole moiety is part of the chemical structure of vitamin B<sub>12</sub> which is one of the biologically relevant natural compounds [1]. Benzimidazole and its derivatives have attracted continuing interest over the years because of their varied biological activities *viz.* anticancer [2], antihypertensive [3], antiviral [4], anti-inflammatory [5], vasodilator [6] and antimicrobial [7–9]. Moreover, as a typical heterocyclic ligand, the large benzimidazole rings not only can provide potential supramolecular recognition sites for  $\pi$ – $\pi$  stacking interactions, but also act as hydrogen bond acceptors and donors to assemble multiple coordination geometry [10].

Transition metal complexes are currently being used to bind and react at specific sequences of DNA in a search for novel chemotherapeutics and probing DNA, and for the development of highly sensitive diagnostic agents [11–13]. Therefore, an understanding that how these small molecules bind to DNA will potentially be useful in the design of such new compounds, which can recognize specific sites or conformations of DNA [12–14]. As both the spectroscopic tags and functional models for the active centers of proteins, metal complexes have helped to elucidate the mechanisms by which metalloproteins function [12]. However, transition metal complexes containing benzimidazole-based ligand are a subject of intensive researches not only owing to their rich coordination chemistry but also due to a number of established and potential

application areas [15,16], which gives the possibility for further research, such as design of structural probes and the development of novel therapeutics.

In the framework of our research project, mainly focus on dealing with the transition metal complexes containing benzimidazole-based ligand and exploring the reaction mechanism with DNA. In preceding reports [17–21], we have investigated the coordinating ability of various benzimidazole ligands and the corresponding transition metal complexes. In this paper, the synthesis, characterization and DNA-binding activities of Ni(II) complex with a V-shape ligand are presented. Moreover, We also conducted an investigation to explore whether the Ni(II) complex has the antioxidant property.

## 2. Experimental section

### 2.1. Materials and methods

All chemicals and solvents were reagent grade and were used without further purification. C, H and N elemental analyses were determined using a Carlo Erba 1106 elemental analyzer. Electrolytic conductance measurements were made with a DDS-307 type conductivity bridge using  $3 \times 10^{-3} \text{ mol L}^{-1}$  solutions in DMF at room temperature. The IR spectra were recorded in the 4000–400  $\text{cm}^{-1}$  region with a Nicolet FT-VERTEX 70 spectrometer using KBr pellets. Electronic spectra were taken on a Lab-Tech UV Bluestar spectrophotometer. The fluorescence spectra were performed on a LS-45 spectrofluorophotometer. The absorbance was measured with Spectrumlab 722sp spectrophotometer at room

\* Corresponding author. Tel.: +86 13893117544.

E-mail address: [wuhuilu@163.com](mailto:wuhuilu@163.com) (H. Wu).

temperature.  $^1\text{H}$  NMR spectra were recorded on a Varian VR300 MHz spectrometer with TMS as an internal standard.

The stock solution of babb and Ni(II) complex were dissolved in DMF at the concentration  $3 \times 10^{-3}$  M. Calf thymus DNA (CT-DNA) and ethidium bromide (EB) were purchased from Sigma. All the experiments involving interaction of the ligand and the complexes with CT-DNA were carried out in doubly distilled water buffer containing 5 mM Tris and 50 mM NaCl and adjusted to pH 7.2 with hydrochloric acid. A solution of CT-DNA gave a ratio of UV absorbance at 260 and 280 nm of about 1.8–1.9, indicating that the CT-DNA was sufficiently free of protein [22]. The CT-DNA concentration per nucleotide was determined spectrophotometrically by employing an extinction coefficient of  $6600 \text{ M}^{-1} \text{ cm}^{-1}$  at 260 nm [23].

Synthetic routine of ligand babb is showed in Scheme 1.

## 2.2. Synthesis

### 2.2.1. Synthesis of ligand: babb

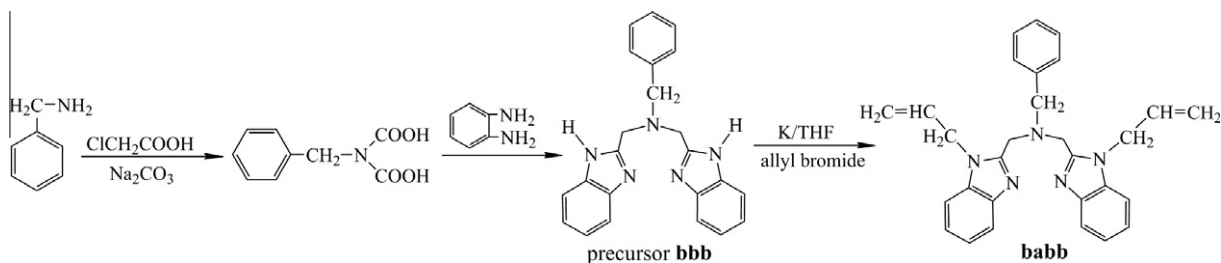
The precursor bis(2-benzimidazol-2-ylmethyl)benzylamine (bbb) was synthesized following a slight modification of the procedure in Ref. [24], bbb (7.34 g, 20 mmol) and potassium (1.56 g, 40 mmol) were put in tetrahydrofuran (150 mL), the solution was refluxed on a water bath for 4 h with stirring. Then, allylbromide (4.84 g, 40 mmol) was added to this solution. With the dropping of allylbromide, the solution gradually becomes cream yellow. After that, the resulting solution was concentrated and cooled, a pale yellow solid separating out and the pale yellow precipitate was filtered, washed with massive water, and recrystallized from ethanol to give the ligand.

Yield: 5.46 g (61%); m.p.: 113–115 °C. Found (%): C, 78.02; H, 6.35; N, 15.71. Calcd. (%) for  $\text{C}_{29}\text{H}_{29}\text{N}_5$ : C, 77.82; H, 6.53; N, 15.65.  $\lambda_m$ (DMF, 297 K):  $1.97 \text{ S cm}^2 \text{ mol}^{-1}$ .  $^1\text{H}$  NMR (DMSO- $d_6$  400 MHz)  $\delta$ /ppm: 3.45 (m, 2H,  $-\text{CH}_2-\text{Ar}$ ), 3.85 (s, 4H,  $-\text{CH}_2-\text{benzimidazol}$ ), 4.87–5.68 (m, 10H,  $-\text{CH}_2-\text{CH}=\text{CH}_2$ ), 7.22 (m, 5H, H-benzene ring), 7.27–7.64 (m, 8H, H-benzimidazol ring). UV-vis ( $\lambda$ , nm): 279, 286. FT-IR (KBr  $\nu/\text{cm}^{-1}$ ): 737,  $\nu(o-\text{Ar})$ ; 1265,  $\nu(\text{C}-\text{N})$ ; 1461,  $\nu(\text{C}=\text{N})$ ; 1643,  $\nu(\text{C}=\text{C})$ .

### 2.2.2. Synthesis of complex: $[\text{Ni}(\text{babb})_2](\text{pic})_2$

To a stirred solution of babb (223.5 mg, 0.50 mmol) in hot EtOH (10 mL) was added Ni(pic) $_2$  (128.73 mg, 0.25 mmol) in EtOH (2 mL). A yellow crystalline product formed rapidly. The precipitate was filtered off, washed with EtOH and absolute Et $_2$ O, and dried under vacuum. The crude product was dissolved in MeCN to form a pale yellow solution into which Et $_2$ O was allowed to diffuse at room temperature. Yellow crystals of it suitable for X-ray measurement were obtained after two weeks.

Yield: 164.7 mg (62%). Found (%): C, 51.41; H, 3.29; N, 16.13. Calcd. (%) for  $\text{C}_{66}\text{H}_{58}\text{N}_{18}\text{O}_{15}\text{Zn}$ : C, 51.17; H, 3.46; N, 16.01.  $\lambda_m$ (DMF, 297 K):  $91.09 \text{ S cm}^2 \text{ mol}^{-1}$ . UV-vis ( $\lambda$ , nm): 279, 282, 381. FT-IR (KBr  $\nu/\text{cm}^{-1}$ ): 746,  $\nu(o-\text{Ar})$ ; 1272,  $\nu(\text{C}-\text{N})$ ; 1365,  $\nu(\text{O}-\text{N}-\text{O})$ ; 1490,  $\nu(\text{C}=\text{N})$ ; 1633,  $\nu(\text{C}=\text{C})$ .



Scheme 1. Synthetic routine of ligand babb.

## 2.3. X-ray crystallography

A suitable single crystal was mounted on a glass fiber, and the intensity data were collected on a Bruker Smart CCD diffractometer with graphite-monochromated Mo- $K_\alpha$  radiation ( $\lambda = 0.71073 \text{ \AA}$ ) at 296 K. Data reduction and cell refinement were performed using the SMART and SAINT programs [25]. The structure was solved by direct methods and refined by full-matrix least-squares against  $F^2$  of data using SHELXTL software [26]. All H atoms were found in difference electron maps and subsequently refined in a riding-model approximation with C–H distances ranging from 0.93 to 0.97  $\text{\AA}$  and  $U_{\text{iso}}(\text{H}) = 1.2 U_{\text{eq}}(\text{C})$ .

## 2.4. DNA-binding experiments

### 2.4.1. Electronic absorption titration

Absorption titration experiments were performed with fixed concentrations of the complexes, while gradually increasing the concentration of CT-DNA. To obtain the absorption spectra, the required amount of CT-DNA was added to both the compound and reference solutions, in order to eliminate the absorbance of CT-DNA itself. From the absorption titration data, the binding constant ( $K_b$ ) was determined using the equation [27]:

$$[\text{DNA}]/(\varepsilon_a - \varepsilon_f) = [\text{DNA}]/(\varepsilon_b - \varepsilon_f) + 1/K_b(\varepsilon_b - \varepsilon_f)$$

where [DNA] is the concentration of CT-DNA in base pairs,  $\varepsilon_a$  corresponds to the observed extinction coefficient ( $A_{\text{obsd}}/[M]$ ),  $\varepsilon_f$  corresponds to the extinction coefficient of the free compound,  $\varepsilon_b$  is the extinction coefficient of the compound when fully bound to CT-DNA, and  $K_b$  is the intrinsic binding constant. The ratio of slope to intercept in the plot of  $[\text{DNA}]/(\varepsilon_a - \varepsilon_f)$  versus [DNA] gave the value of  $K_b$ .

### 2.4.2. Fluorescence studies

The enhanced fluorescence of EB in the presence of DNA can be quenched by the addition of a second molecule [28,29]. The extent of fluorescence quenching of EB bound to CT-DNA can be used to determine the extent of binding between the second molecule and CT-DNA. Competitive binding experiments were carried out in the buffer by keeping  $[\text{DNA}]/[\text{EB}] = 1$  and varying the concentrations of the compounds. The fluorescence spectra of EB were measured using an excitation wavelength of 520 nm, and the emission range was set between 550 and 750 nm. The spectra were analyzed according to the classical Stern–Volmer equation [30]:

$$I_0/I = 1 + K_{\text{sv}}[\text{Q}]$$

where  $I_0$  and  $I$  are the fluorescence intensities at 599 nm in the absence and presence of the quencher, respectively,  $K_{\text{sv}}$  is the linear Stern–Volmer quenching constant, and [Q] is the concentration of the quencher. In these experiments  $[\text{CT-DNA}] = 2.5 \times 10^{-3} \text{ mol/L}$ ,  $[\text{EB}] = 2.2 \times 10^{-3} \text{ mol/L}$ .

### 2.4.3. Viscosity titration measurements

Viscosity experiments were conducted on an Ubbelohde viscometer, immersed in a water bath maintained at  $25.0 \pm 0.1$  °C. Titrations were performed for the complexes (3–30  $\mu\text{M}$ ), and each compound was introduced into CT-DNA solution (42.5  $\mu\text{M}$ ) present in the viscometer. Data were analyzed as  $(\eta/\eta_0)^{1/3}$  versus the ratio of the concentration of the compound to CT-DNA, where  $\eta$  is the viscosity of CT-DNA in the presence of the compound and  $\eta_0$  is the viscosity of CT-DNA alone. Viscosity values were calculated from the observed flow time of CT-DNA-containing solutions corrected from the flow time of buffer alone ( $t_0$ ),  $\eta = (t - t_0)$  [31].

### 2.5. Antioxidant property

Hydroxyl radicals were generated in aqueous media through the Fenton-type reaction [32,33]. The aliquots of reaction mixture (3 mL) contained 1.0 mL of 0.10 mmol aqueous safranin, 1 mL of 1.0 mmol aqueous EDTA-Fe(II), 1 mL of 3% aqueous  $\text{H}_2\text{O}_2$ , and a series of quantitative microadditions of solutions of the test compound. A sample without the tested compound was used as the control. The reaction mixtures were incubated at 37 °C for 30 min in a water bath. The absorbance was then measured at 520 nm. All the tests were run in triplicate and are expressed as the mean and standard deviation (SD) [34]. The scavenging effect for  $\text{OH}\cdot$  was calculated from the following expression:

$$\text{Scavenging ratio (\%)} = [(A_i - A_0)/(A_c - A_0)] \times 100\%$$

where  $A_i$  is the absorbance in the presence of the test compound;  $A_0$  is absorbance of the blank in the absence of the test compound;  $A_c$  is the absorbance in the absence of the test compound, EDTA-Fe(II) and  $\text{H}_2\text{O}_2$ .

## 3. Results and discussion

Ligand babb and its Ni(II) complex are very stable in the air. Ni(II) complex is remarkably soluble in polar aprotic solvents such as DMF, DMSO and MeCN; slightly soluble in ethanol, methanol, ethyl acetate and chloroform; insoluble in water,  $\text{Et}_2\text{O}$ , and petroleum ether. The molar conductivities in DMF solution indicate that babb is a nonelectrolyte while Ni(II) complex is a 1:2 electrolyte compound [35].

### 3.1. IR and electronic spectra

The IR spectra of the Ni(II) complex is closely related to that of the free ligand babb. One of the most diagnostic changes occurs in the region between 1650 and 1250  $\text{cm}^{-1}$ . The spectra of babb show a strong band at 1461  $\text{cm}^{-1}$  and weak bands at 1643  $\text{cm}^{-1}$ . By analogy with the assigned bands of imidazole, two bands are attributed to the  $\nu(\text{C}=\text{N})$  and  $\nu(\text{C}=\text{C})$  frequencies of the benzimidazole group, respectively [36–38]. The band  $\nu(\text{C}=\text{N})$  undergo a blue shift (about 29 nm) in the complex as compared to free ligand indicating the participation of the imine nitrogen atoms in coordination to the metal ion [39]; these are the preferred nitrogen atom for coordination, as found in other metal complexes with benzimidazoles [40]. Moreover, Information regarding the possible bonding modes of the picrate and benzimidazole rings may also be obtained from the IR spectra [41].

DMF solutions of ligand and Ni(II) complex show, as expected, almost identical UV spectra. The UV bands of babb (286, 279 nm) are only marginally red-shifted about 4 nm for Ni(II) complex, which is evidence of  $\text{C}=\text{N}$  coordination to the metal center. These bands are assigned to  $\pi \rightarrow \pi^*$  (imidazole) transitions. The picrate bands (observed at 381 nm) are assigned to  $\pi \rightarrow \pi^*$  transitions [17,18].

### 3.2. X-ray structures of the complexes

Basic crystal data, description of the diffraction experiment, and details of the structure refinement are given in Table 1. Selected bond distances and angles are presented in Table 2.

#### 3.2.1. The crystal structure of complex: $[\text{Ni}(\text{babb})_2](\text{pic})_2$

The crystal structure of Ni(II) complex consists of a discrete  $[\text{Ni}(\text{babb})_2]^{2+}$  cation, two picrate anions. The ORTEP structure (30% probability ellipsoids) of the  $[\text{Ni}(\text{babb})_2]^{2+}$  with atom-numberings is shown in Fig. 1.

The central Ni(II) atom is six-coordinated with a  $\text{N}_6$  ligand set, in which six nitrogen atoms afforded by two tridentate ligand babb. The coordination geometry of the Ni(II) may be best described as distorted octahedral with (N1, N3, N7, N9) providing the equatorial plane. The maximum deviation distance (N3) from the least squares plane calculated from the four coordination atom atoms is 0.241 Å, and the nickel atom is out of this plane by only 0.133 Å. The distance between the axial atom N5, N6 and the equatorial plane are 2.138 Å, 2.075 Å, respectively. The bond angle of the two atoms (N5–Ni–N6) in axial positions is 167.76(12)°. Therefore, compared with a regular octahedron, it reflects a relatively distorted coordination octahedron around central Ni(II) atom [42–45].

### 3.3. DNA binding properties

#### 3.3.1. Absorption spectroscopic studies

The application of electronic absorption spectra in DNA-binding studies is one of the most useful techniques. The binding of intercalative drugs to DNA has been characterized classically through absorption titrations, following the hypochromism and red shift associated with binding of the colored complex to the helix [27]. The absorption spectra of the ligand babb and Ni(II) complex in the absence and presence of CT-DNA (at a constant concentration of compounds) are given in Fig. 2. With increasing DNA concentrations, the hypochromism reaches as high as 18.32% at 275 nm for free li-

**Table 1**  
Crystal data and structure refinement for  $[\text{Ni}(\text{babb})_2](\text{pic})_2$ .

Complex	$[\text{Ni}(\text{babb})_2](\text{pic})_2$
Molecular formula	$\text{C}_{70}\text{H}_{62}\text{N}_{16}\text{NiO}_{14}$
Molecular weight	1410.07
Color	Yellow
Crystal size, mm <sup>3</sup>	$0.36 \times 0.34 \times 0.30$
Crystal system	Triclinic
Space group	<i>P</i> -1
<i>a</i> (Å)	13.877(3)
<i>b</i> (Å)	13.945(3)
<i>c</i> (Å)	19.172(4)
$\alpha$ (°)	70.138(2)
$\beta$ (°)	88.891(2)
$\gamma$ (°)	74.189(2)
<i>V</i> (Å <sup>3</sup> )	3346.3(12)
<i>Z</i>	2
<i>T</i> (K)	293(2)
<i>D</i> <sub>calcd</sub> (g cm <sup>-3</sup> )	1.399
<i>F</i> (000) (e)	1468
$\theta$ range for data collection (°)	2.27–25.00
<i>hkl</i> range	$-16 \leq h \leq 13$ , $-16 \leq k \leq 16$ , $-22 \leq l \leq 22$
Reflections collected	20973
Independent reflections	11596 [ <i>R</i> <sub>int</sub> = 0.0328]
Refinement method	Full-matrix least-squares on <i>F</i> <sup>2</sup>
Data/restraints/parameters	11596/35/910
Final <i>R</i> <sub>1</sub> / <i>wR</i> <sub>2</sub> indices [ <i>I</i> ≥ 2σ( <i>I</i> )] <sup>a</sup>	0.0598/0.1526
<i>R</i> <sub>1</sub> / <i>wR</i> <sub>2</sub> indices (all data) <sup>a</sup>	0.0998/0.1811
Goodness-of-fit on <i>F</i> <sup>2</sup>	1.018
Largest diff. peak and hole (e Å <sup>-3</sup> )	0.852 and -0.616

**Table 2**  
Selected bond distances (Å) and angles (°) in [Ni(babb)<sub>2</sub>](pic)<sub>2</sub>.

Complex	[Ni(babb) <sub>2</sub> ](pic) <sub>2</sub>			
Bond distances	Ni(1)–N(1)	2.405(3)	Ni(1)–N(6)	2.310(3)
	Ni(1)–N(3)	2.142(3)	Ni(1)–N(7)	2.127(3)
	Ni(1)–N(5)	2.048(3)	Ni(1)–N(9)	2.082(3)
Bond angles	N(5)–Ni(1)–N(9)	99.88(13)	N(7)–Ni(1)–N(6)	75.14(11)
	N(5)–Ni(1)–N(7)	93.86(12)	N(3)–Ni(1)–N(6)	91.50(12)
	N(9)–Ni(1)–N(7)	104.60(12)	N(5)–Ni(1)–N(1)	76.74(12)
	N(5)–Ni(1)–N(3)	100.72(13)	N(9)–Ni(1)–N(1)	166.23(11)
	N(9)–Ni(1)–N(3)	94.79(13)	N(7)–Ni(1)–N(1)	89.02(11)
	N(7)–Ni(1)–N(3)	153.35(12)	N(3)–Ni(1)–N(1)	73.02(12)
	N(5)–Ni(1)–N(6)	167.76(12)	N(6)–Ni(1)–N(1)	107.89(11)
	N(9)–Ni(1)–N(6)	78.21(12)		

gand babb; 43.90% at 273 nm for complex Ni(II) complex. The  $\lambda_{\max}$  for babb and Ni(II) complex have a slight red shifts of about 1–2 nm under identical experimental conditions. The hypochromism and red shift suggested that the babb and Ni(II) complex have strong interaction with DNA [46]. The  $K_b$  values of babb and Ni(II) complex are  $2.26 \times 10^3 \text{ M}^{-1}$  ( $R = 0.98$  for 15 points),  $3.65 \times 10^4 \text{ M}^{-1}$  ( $R = 0.99$  for 16 points) for Ni(II) complex, respectively. Therefore, compare with the classic DNA-intercalative reagent, such as Ethidium bromide (EB), acridine orange (AO), methylene blue (MB) [47], in the light of the hypochromism and red shift mentioned above, we speculate that ligand babb and Ni(II) complex most possibly binds to DNA in an intercalation mode, which may due to the large coplanar aromatic rings in two compound that facilitate it intercalating to the base pairs of double helical DNA.

However, the affinity for DNA is more strong in case of Ni(II) complex when compared with the ligand. For this difference, we attributed to three possible reasons. (i) By comparison of the molecular structure of the ligand and Ni(II) complex, we find the greater number of coplanar aromatic rings may lead to higher

affinity for DNA [48]. (ii) The charge transfer of coordinated babb ligands caused by the coordination of the central Ni(II) atom, lead to the reduce of the charge density of the plane conjugate system, which is conducive to insert. (iii) This difference in their DNA binding ability also could be attributed to the presence of an electron deficient center in the charged Ni(II) complex where an additional interaction between the complex and phosphate rich DNA backbone may occur [49,50].

### 3.3.2. Fluorescence spectroscopic studies

In order to further study the binding properties of the complexes with DNA, competitive binding experiment was carried out. Relative binding of babb and Ni(II) complex to CT-DNA was studied by the fluorescence spectral method using ethidium bromide (EB) bound CT-DNA solution in Tris–HCl/NaCl buffer (pH = 7.2). As a typical indicator of intercalation, EB is a weakly fluorescent compound. But in the presence of DNA, emission intensity of EB is greatly enhanced because of its strong intercalation between the adjacent DNA base pairs [29]. In general, measurement of the ability of a complex to affect the intensity of EB fluorescence in the EB-DNA adduct allows determination of the affinity of the complex for DNA, whatever the binding mode may be. If a complex can displace EB from DNA, the fluorescence of the solution will be reduced due to the fact that free EB molecules are readily quenched by the solvent water [51]. For babb and Ni(II) complex, no emission were observed either alone or in the presence of CT-DNA in the buffer. The fluorescence quenching of DNA-bound EB by ligand babb and complex are shown in Fig. 3. The behavior of babb and Ni(II) complex are in good agreement with the Stern–Volmer equation, which provide further evidence that them bind to DNA. The  $K_{sv}$  values are  $1.44 \times 10^4 \text{ M}^{-1}$  ( $R = 0.97$  for 13 points) for babb,  $5.26 \times 10^4 \text{ M}^{-1}$  ( $R = 0.98$  for 10 points in the linear part) for Ni(II) complex, respectively. It may be due to ligand babb and Ni(II) complex both can interact with DNA in an intercalation mode, and releasing

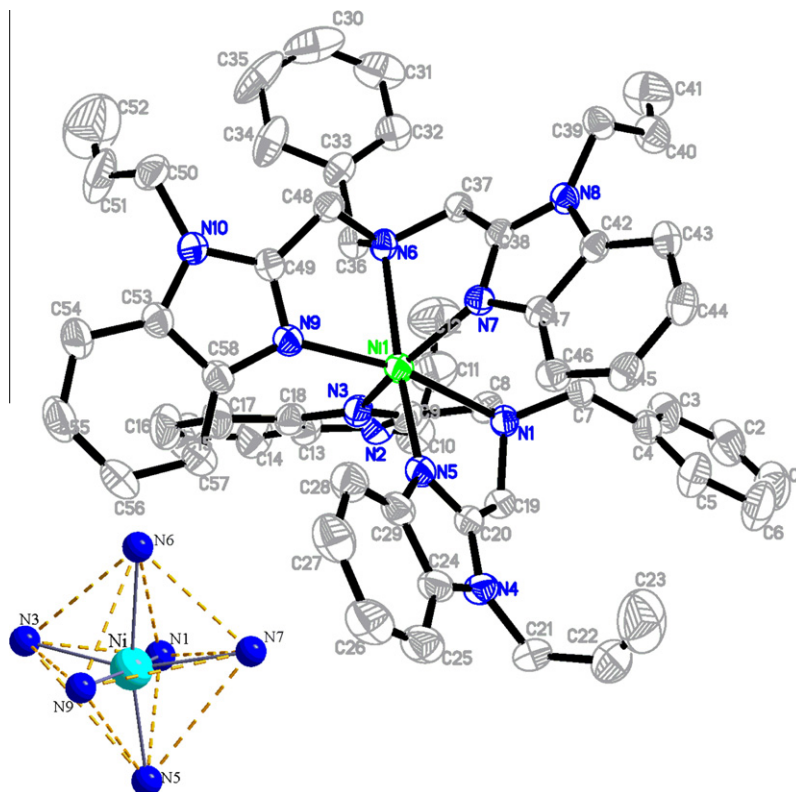


**Fig. 1.** Molecular structure and atom numberings of [Ni(babb)<sub>2</sub>]<sup>2+</sup> with hydrogen atoms were omitted for clarity.

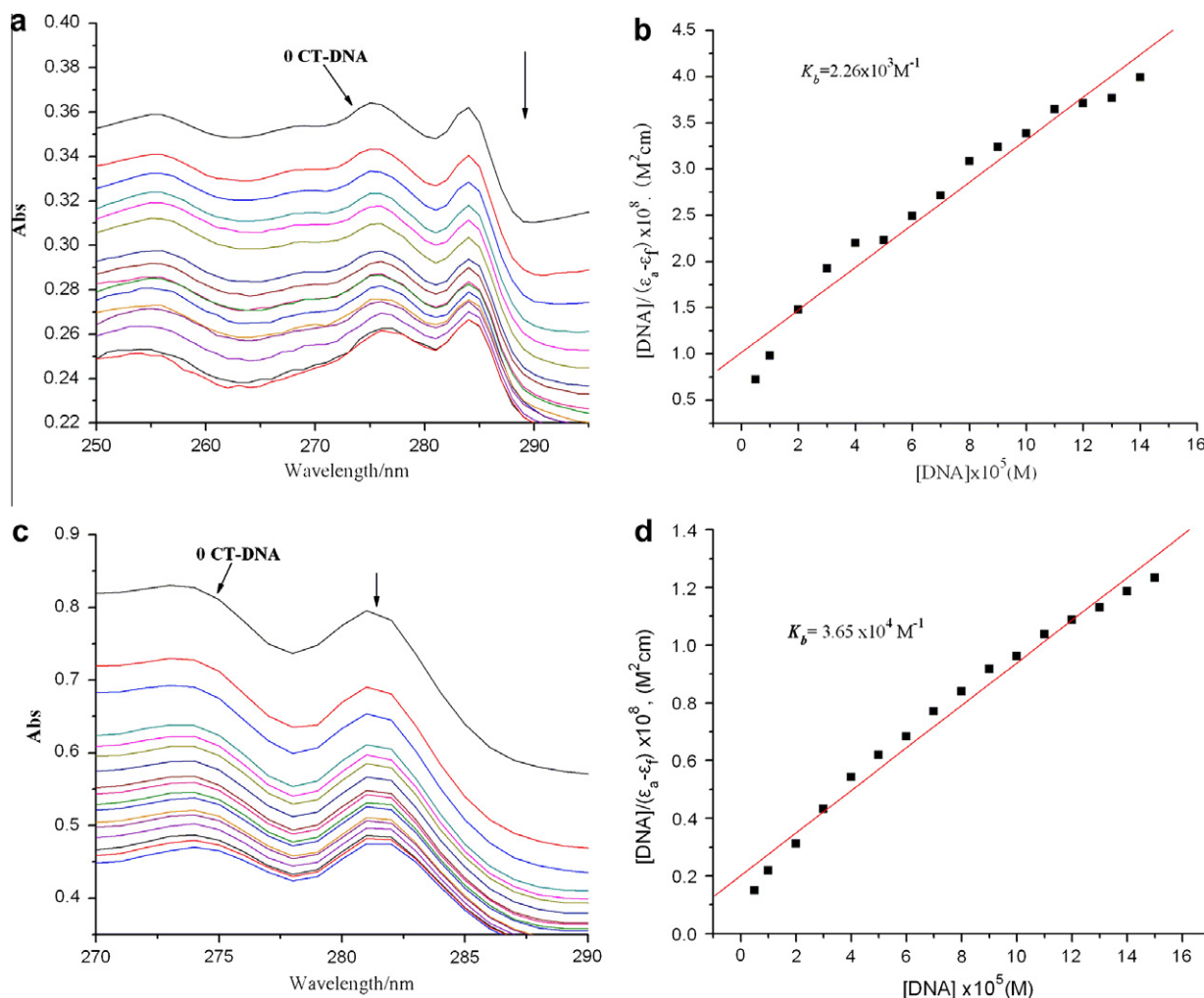


**Fig. 2.** Electronic spectra of (a) babb, (c) Ni(II) complex in Tris-HCl buffer upon addition of CT-DNA. [Compound] =  $3 \times 10^{-5} \text{ M}^{-1}$ , [DNA] =  $2.5 \times 10^{-5} \text{ M}^{-1}$ . Arrow shows the emission intensity changes upon increasing DNA concentration. Plots of  $[\text{DNA}]/(\epsilon_0 - \epsilon_t)$  versus  $[\text{DNA}]$  for the titration of (b) babb, (d) Ni(II) complex with CT-DNA.

some free EB from the EB-bound CT-DNA complex system and that DNA-binding of Ni(II) complex is stronger than that of babb, which is consistent with the above absorption spectroscopic results. The  $K_q$  values for the ligand babb and the Ni(II) complex are  $1.44 \times 10^{12} \text{ M}^{-1} \text{ S}^{-1}$  and  $5.26 \times 10^{12} \text{ M}^{-1} \text{ S}^{-1}$ , respectively, indicating they are static quenching [52].

### 3.3.3. Viscosity titration measurements

Optical photophysical techniques are widely used to study the binding model of the ligand, metal complexes and DNA, but do not give sufficient clues to support a binding model. Hydrodynamic measurements that are sensitive to the length change (i.e., viscosity and sedimentation) are regarded as the least ambiguous and the most critical tests of a binding model in solution in the absence of crystallographic structural data [22,53]. Therefore, viscosity measurements were carried out to further clarify the interaction of metal complexes and DNA. In classical intercalation, the DNA helix lengthens as base pairs are separated to accommodate the bound ligand leading to increased DNA viscosity whereas a partial, while nonclassical ligand intercalation causes a bend (or kink) in DNA helix reducing its effective length and thereby its viscosity [22].

The effects of babb and Ni(II) complex on the viscosity of CT-DNA is shown in Fig. 4. The viscosity of CT-DNA is increased

steadily with the increment of them, and it is further illustrated that two compounds can intercalate with CT-DNA. The result of the viscosity experiments confirms the mode of babb and Ni(II) complex intercalate into DNA base pairs already established through absorption and fluorescence spectral titration studies.

### 3.4. Antioxidant property

According to relevant reports in the literature [54–56], some transition metal complexes may exhibit antioxidant activity. We therefore also conducted an investigation to explore whether the Ni(II) complex has the hydroxyl radical scavenging property. We compared the abilities of one present compounds to scavenge hydroxyl radicals with those of the well-known natural antioxidants mannitol and vitamin C, using the same method as reported in a previous paper [57]. The 50% inhibitory concentration ( $\text{IC}_{50}$ ) value of mannitol and vitamin C are about  $9.6 \times 10^{-3}$  and  $8.7 \times 10^{-3} \text{ M}^{-1}$ , respectively. As shown in Fig. 5, according to the antioxidant experiments, the  $\text{IC}_{50}$  values of Ni(II) complex is  $6.73 \times 10^{-5} \text{ M}^{-1}$ , which implies that Ni(II) complex has the preferable ability to scavenge hydroxyl radical. In view of the observed  $\text{IC}_{50}$  values, the Ni(II) complex can be considered as a potential drug to eliminate the hydroxyl radical.

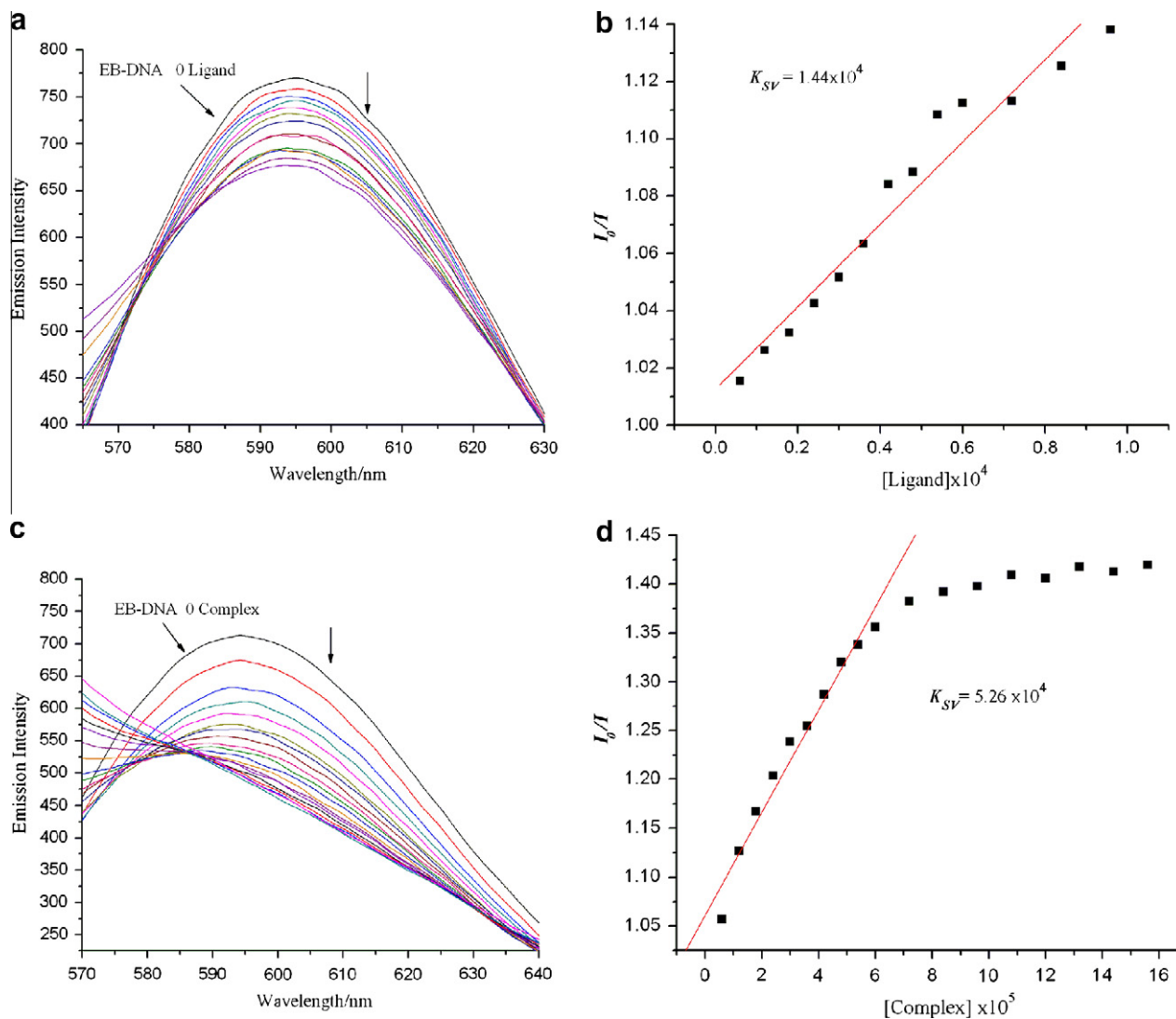


**Fig. 3.** Emission spectra of EB bound to CT-DNA in the presence of (a) babb and (c) Ni(II) complex; [Compound] =  $3 \times 10^{-5}$  M;  $\lambda_{ex}$  = 520 nm. The arrows show the intensity changes upon increasing concentrations of the complexes. Fluorescence quenching curves of EB bound to CT-DNA by (b) ligand and (d) Ni(II) complex. (Plots of  $I_0/I$  versus [Complex]).

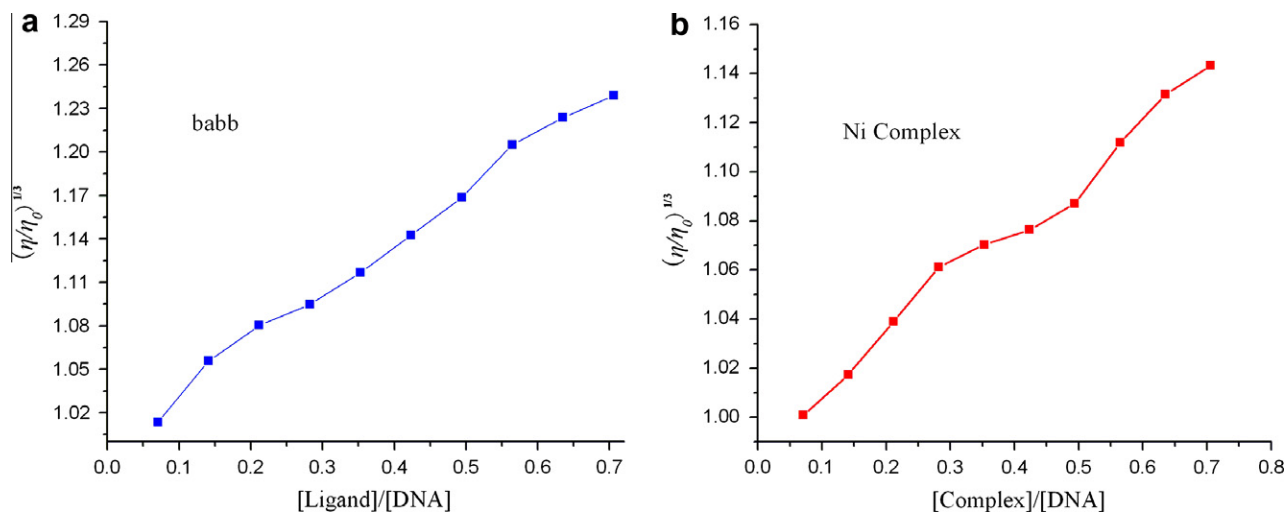


**Fig. 4.** Effect of increasing amounts of (a) babb and (b) Ni(II) complex on the relative viscosity of CT-DNA at  $25.0 \pm 0.1$  °C.

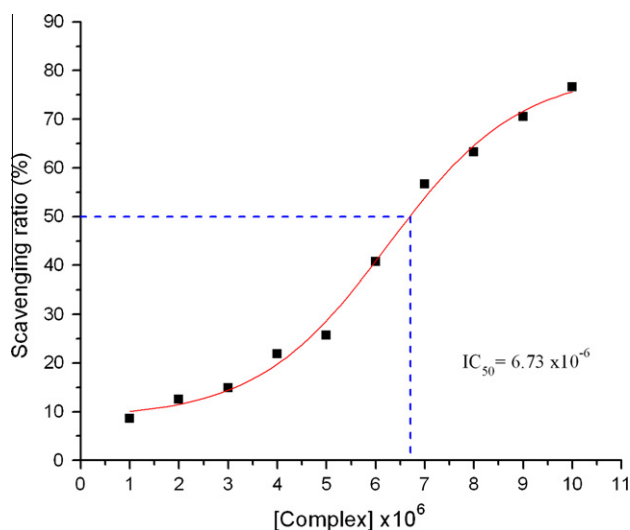


Fig. 5. The inhibitory effect of Ni(II) complex on OH radicals; the suppression ratio increases with increasing concentration of the test compound.

#### 4. Conclusion

In this work, a new ligand bis(*N*-allylbenzimidazol-2-ylmethyl)-benzylamine and its Ni(II) complex have been synthesized and characterized. The crystal structure of [Ni(babb)<sub>2</sub>](pic)<sub>2</sub> is six-coordinated adopting a distorted octahedral geometry. The DNA-binding experimental results suggest that ligand babb and Ni(II) complex bind to DNA in an intercalation mode, and the Ni(II) complex has higher binding ability than free ligand. In addition, the Ni(II) complex can be considered as a potential drug to eliminate the hydroxyl radical. These findings indicate that the Ni(II) complex has many potential practical applications for the development of nucleic acid molecular probes and new therapeutic reagents for diseases on the molecular level and warrant further in vivo experiments and pharmacological assays.

#### Acknowledgments

The authors acknowledge the financial support and grant from 'Qing Lan' Talent Engineering Funds by Lanzhou Jiaotong University. The grant from 'Long Yuan Qing Nian' of Gansu Province also is acknowledged.

#### Appendix A. Supplementary material

Crystallographic data (excluding structure factors) for the structures reported in this paper have been deposited with the Cambridge Crystallographic Data Center with reference number CCDC 848157. Copies of the data can be obtained, free of charge, on application to the CCDC, 12 Union Road, Cambridge CB2 1EZ, UK. Tel.: +44 01223 762910; fax: +44 01223 336033; e-mail: deposit@ccdc.cam.ac.uk or <http://www.ccdc.cam.ac.uk>. Supplementary data associated with this article can be found, in the online version, at doi: 10.1016/j.jphotobiol.2011.11.010.

#### References

- [1] J.B. Wright, The chemistry of the benzimidazoles, *Chem. Rev.* 48 (1951) 397–541.
- [2] S.Y. Hong, K.W. Kwak, C.K. Ryu, S.J. Kang, K.H. Chung, Antiproliferative effects of 6-anilino-5-chloro-1H-benzo[d]imidazole-4,7-dione in vascular smooth muscle cells, *Bioorg. Med. Chem.* 16 (2008) 644–649.
- [3] J.Y. Xu, Y. Zeng, Q. Ran, Z. Wei, Y. Bi, Q.H. He, Q.J. Wang, S. Hu, J. Zhang, M.Y. Tang, W.Y. Hua, X.M. Wu, Synthesis and biological activity of 2-

- alkylbenzimidazoles bearing a *N*-phenylpyrrole moiety as novel angiotensin II AT1 receptor antagonists, *Bioorg. Med. Chem. Lett.* 17 (2007) 2921–2926.
- [4] P.D. Patel, M.R. Patel, N. Kaushik-Basu, T.T. Talele, 3D QSAR and molecular docking studies of benzimidazole derivatives as hepatitis C virus NS5B polymerase Inhibitors, *J. Chem. Inf. Model.* 48 (2008) 42–55.
- [5] K. Taniguchi, S. Shigenaga, T. Ogahara, T. Fujitsu, M. Matsuo, Synthesis and anti-inflammatory and analgesic properties of 2-amino-1H-benzimidazole and 1,2-dihydro-2-iminocycloheptimidazole derivatives, *Chem. Pharm. Bull.* 41 (1993) 301–309.
- [6] S. Estrada-Soto, R. Villalobos-Molina, F. Aguirre-Crespo, J. Vergara-Galicia, H. Oreno-Díaz, M. Torres-Piedra, G. Navarrete-Vázquez, Relaxant activity of 2-(substituted phenyl)-1H-benzimidazoles on isolated rat aortic rings: design and synthesis of 5-nitro derivatives, *Life Sci.* 79 (2006) 430–435.
- [7] Ö.Ö. Guven, T. Erdoğan, H. Göker, S. Yildiz, Synthesis and antimicrobial activity of some novel phenyl and benzimidazole substituted benzyl ethers, *Bioorg. Med. Chem. Lett.* 17 (2007) 2233–2236.
- [8] Z. Ates-Alagoz, S. Yildiz, E. Buyukbingol, Antimicrobial activities of some tetrahydronaphthalene-benzimidazole derivatives, *Chemotherapy* 53 (2007) 110–113.
- [9] B.G. Mohamed, A.A. Abdel-Alim, M.A. Hussein, Synthesis of 1-acyl-2-alkylthio-1,2,4-triazolobenzimidazoles with antifungal, anti-inflammatory and analgesic effects, *Acta Pharm.* 56 (2006) 31–48.
- [10] H.Y. Liu, H. Wu, J. Yang, Y.Y. Liu, B. Liu, Y.Y. Liu, J.F. Ma, pH-Dependent assembly of 1D to 3D octamolybdate hybrid materials based on a new flexible bis-(pyridyl)-benzimidazole ligand, *Cryst. Growth Des.* 11 (2011) 2920–2927.
- [11] M.S. Diaz-Cruz, J. Mendieta, A. Monjonelli, R. Tauler, M. Esteban, Specific interactions of bovine and human  $\beta$ -casomorphin-7 with Cu(II) ions, *J. Inorg. Biochem.* 70 (1998) 91–95.
- [12] K.E. Erkkila, D.T. Odom, J.K. Barton, Recognition and reaction of metallointercalators with DNA, *Chem. Rev.* 99 (1999) 2777–2796.
- [13] L.N. Ji, X.H. Zou, J.G. Lin, Shape- and enantioselective interaction of Ru(II)/Co(III) polypyridyl complexes with DNA, *Coord. Chem. Rev.* 216–217 (2001) 513–536.
- [14] B.M. Zeglis, V.C. Pierre, J.K. Barton, Metallo-intercalators and metallo-insertors, *Chem. Commun.* 44 (2007) 4565–4579.
- [15] J.A. Cowan, Metal activation of enzymes in nucleic acid biochemistry, *Chem. Rev.* 98 (1998) 1067–1088.
- [16] C.L. Liu, M. Wang, T.L. Zhang, H.Z. Sun, DNA hydrolysis promoted by di- and multi-nuclear metal complexes, *Coord. Chem. Rev.* 248 (2004) 147–168.
- [17] H.L. Wu, X.C. Huang, J.K. Yuan, F. Kou, F. Jia, B. Liu, K.T. Wang, A V-shaped ligand 2,6-bis(2-benzimidazolyl)pyridine and its picrate Mn(II) complex: Synthesis, crystal structure and DNA-binding properties, *Eur. J. Med. Chem.* 45 (2010) 5324–5330.
- [18] H.L. Wu, K. Li, T. Sun, F. Kou, F. Jia, J.K. Yuan, B. Liu, B.L. Qi, Synthesis, structure, and DNA-binding properties of manganese(II) and zinc(II) complexes with tris(*N*-methylbenzimidazol-2-ylmethyl)amine ligand, *Transition. Met. Chem.* 36 (2011) 21–28.
- [19] H.L. Wu, R.R. Yun, K.T. Wang, K. Li, X.C. Huang, T. Sun, Synthesis, crystal structure, and spectrum properties of cobalt(II) complexes based on tridentate 1, 3-bis(benzimidazol-2-yl)-2-oxopropane ligand and derivative, *Z. Anorg. Allg. Chem.* 636 (2010) 629–633.
- [20] H.L. Wu, X.C. Huang, J.K. Yuan, K. Li, J. Ding, R.R. Yun, W.K. Dong, X.Y. Fan, A five-coordinate copper(II) perchlorate complex with tris(*N*-methylbenzimidazol-2-ylmethyl)amine and salicylate, *J. Coord. Chem.* 62 (2009) 3446–3453.
- [21] H.L. Wu, J.K. Yuan, Y. Bai, F. Kou, F. Jia, B. Liu, Synthesis crystal structure and spectra properties of the cadmium (II) complex with bis(*N*-allylbenzimidazol-2-ylmethyl)benzylamine, *Bioinorg. Chem. Appl.* 2011 (2011) 705989.
- [22] S. Satyanarayana, J.C. Dabrowiak, J.B. Chaires, Tris(phenanthroline)-ruthenium(II) enantiomer interactions with DNA: mode and specificity of binding, *Biochemistry* 32 (1993) 2573–2584.
- [23] M.E. Reichmann, S.A. Rice, C.A. Thomas, P. Doty, A further examination of the molecular weight and size of desoxyribose nucleic acid, *J. Am. Chem. Soc.* 76 (1954) 3047–3051.
- [24] K. Takahashi, Y. Nishida, S. Kida, Crystal structure of copper(II) complex with *N*, *N*-bis(2-benzimidazolylmethyl)benzylamine, *Polyhedron* 3 (1984) 113–116.
- [25] Bruker, Smart saint and sadabs, Bruker Axs, Inc., Madison, WI, 2000.
- [26] G.M. Sheldrick, SHELXTL, Siemens Analytical X-ray Instruments, Inc., Madison, Wisconsin, USA, 1996.
- [27] A.M. Pyle, J.P. Rehmann, R. Meshoyrer, C.V. Kumar, N.J. Turro, J.K. Barton, Mixed-ligand complexes of ruthenium(II): factors governing binding to DNA, *J. Am. Chem. Soc.* 111 (1989) 3051–3058.
- [28] A. Wolf, G.H. Shimer, T. Meehan, Polycyclic aromatic hydrocarbons physically intercalate into duplex regions of denatured DNA, *Biochemistry* 26 (1987) 6392–6396.
- [29] B.C. Baguley, M.L. Bret, Quenching of DNA-ethidium fluorescence by amsacrine and other antitumor agents: a possible electron-transfer effect, *Biochemistry* 23 (1984) 937–943.
- [30] J.R. Lakowicz, G. Webber, Quenching of fluorescence by oxygen Probe for structural fluctuations in macromolecules, *Biochemistry* 12 (1973) 4161–4170.
- [31] C.P. Tan, J. Liu, L.M. Chen, S. Shi, L.N. Ji, Synthesis, structural characteristics, DNA binding properties and cytotoxicity studies of a series of Ru(III) complexes, *J. Inorg. Biochem.* 102 (2008) 1644–1653.
- [32] C.C. Winterbourn, Hydroxyl radical production in body fluids. Roles of metal ions, ascorbate and superoxide, *Biochem. J.* 198 (1981) 125–131.

- [33] C.C. Winterbourn, Comparison of superoxide with other reducing agents in the biological production of hydroxyl radicals, *Biochem. J.* 182 (1979) 625–628.
- [34] Z.Y. Guo, R.E. Xing, S. Liu, H.H. Yu, P.B. Wang, C.P. Li, P.C. Li, The synthesis and antioxidant activity of the Schiff bases of chitosan and carboxymethyl chitosan, *Bioorg. Med. Chem. Lett.* 15 (2005) 4600–4603.
- [35] W.J. Geary, The use of conductivity measurements in organic solvents for the characterization of coordination compounds, *Coord. Chem. Rev.* 7 (1971) 81–122.
- [36] C.Y. Su, B.S. Kang, C.X. Du, Q.C. Yang, T.C.W. Mak, Formation of mono-, bi-, tri-, and tetranuclear Ag(I) complexes of  $C_3$ -symmetric tripodal benzimidazole ligands, *Inorg. Chem.* 39 (2000) 4843–4849.
- [37] T.J. Lane, I. Nakagawa, J.L. Walter, A.J. Kandathil, Infrared investigation of certain imidazole derivatives and their metal chelates, *Inorg. Chem.* 1 (1962) 267–276.
- [38] E.K. Chec, M. Kubiak, T. Glowiak, J.J. Ziolkowski, Synthesis, crystal and molecular structure of the novel complex [dinitrato{N, N-bis(1-methylbenzimidazol-2-ylmethyl)methylamine}]cobalt(II), *Transition. Met. Chem.* 23 (1998) 641–644.
- [39] M. McKee, M. Zvagulis, C.A. Reed, Further insight into magnetostructural correlations in binuclear copper(II) species related to methemoglobin: x-ray crystal structure of 1, 2- $\mu$ -nitrito complex, *Inorg. Chem.* 24 (1985) 2914–2919.
- [40] K. Nakamoto (Ed.), *Infrared and Raman Spectra of Inorganic and Coordination Compounds*, Wiley, New York, 1978, p. 305.
- [41] H.L. Wu, K.T. Wang, R.R. Yun, X.C. Huang, Studies on copper(II), cobalt (II) and nickel (II) picrate complexes with the ligand 1,3-bis(2-benzimidazolyl)-2-thiapropane, *Synth. React. Inorg., Met.-Org., Nano-Met. Chem.* 39 (2009) 629–632.
- [42] L.E. Xiao, M. Zhang, W.H. Sun, Synthesis, characterization and ethylene oligomerization and polymerization of 2-(1H-2-benzimidazolyl)-6-(1-(arylimino)ethyl)pyridylchromium chlorides, *Polyhedron* 29 (2010) 142–147.
- [43] D. Kang, J. Seo, S.Y. Lee, J.Y. Lee, First dicadmium(II) complex of tripodal amide ligand with one edge-sharing monocapped octahedral geometry, *Inorg. Chem. Commun.* 10 (2007) 1425–1428.
- [44] N. Yoshikawa, S. Yamabe, N. Kanehisa, Y. Kai, H. Takashima, K. Tsukahara, Synthesis, characterization, and DFT investigation of Ir(III) tolylterpyridine complexes, *Eur. J. Inorg. Chem.* 13 (2007) 1911–1919.
- [45] J.P. Collin, I.M. Dixon, J.P. Sauvage, J.A.G. Williams, F. Barigelli, L. Flamigni, Synthesis and photophysical properties of Iridium(III) bisterpyridine and its homologues: a family of complexes with a long-lived excited state, *J. Am. Chem. Soc.* 121 (1999) 5009–5016.
- [46] J. Liu, T.X. Zhang, L.N. Ji, DNA-binding and cleavage studies of macrocyclic copper(II) complexes, *J. Inorg. Biochem.* 91 (2002) 269–276.
- [47] S. Nafisi, A.A. Saboury, N. Keramat, J.F. Neault, H.A. Tajmir-Riahi, Stability and structural features of DNA intercalation with ethidium bromide, acridine orange and methylene blue, *J. Mol. Struct.* 827 (2007) 35–43.
- [48] H.L. Wu, J.K. Yuan, Y. Bai, F. Jia, B. Liu, F. Kou, J. Kong, Synthesis, structure, DNA-binding properties, and antioxidant activity of copper(II) and cobalt(II) complexes with bis(N-allylbenzimidazol-2-ylmethyl)benzylamine, *Transition. Met. Chem.* 36 (2011) 819–827.
- [49] S. Yellappa, J. Seetharamappa, L.M. Rogers, R. Chitta, R.P. Singhal, F. D'Souza, Binding, electrochemical activation, and cleavage of DNA by cobalt(II)tetrakis-N-methylpyridyl porphyrin and its b-pyrrole brominated derivative, *Bioconjug. Chem.* 17 (2006) 1418–1425.
- [50] M. Shakir, M. Azam, M.-F. Ullah, S.-M. Hadi, Synthesis, spectroscopic and electrochemical studies of N, N-bis[(E)-2-thienylmethylidene]-1,8-naphthalene -diamine and its Cu(II) complex: DNA cleavage and generation of superoxide anion, *J. Photoch. Photobio. B* 104 (2011) 449–456.
- [51] J.B. LePecq, C. Paoletti, A fluorescent complex between ethidium bromide and nucleic acids: Physical–Chemical characterization, *J. Mol. Biol.* 27 (1967) 87–106.
- [52] Q.H. Zhou, P. Yang, Synthesis, crystal structure and DNA binding studies of Zn(II) complex with 1,3-bis(benzimidazol-2-yl)-2-oxapropane, *Acta Chim. Sinica* 64 (2006) 793–798.
- [53] S. Satyanarayana, J.C. Dabroniak, J.B. Chaires, Neither DELTA- nor LAMBDA-tris(phenanthroline)ruthenium(II) binds to DNA by classical intercalation, *Biochemistry* 31 (1992) 9319–9324.
- [54] S.B. Bukhari, S. Memon, M. Mahroof-Tahir, M.I. Bhaner, Synthesis, characterization and antioxidant activity copper–quercetin complex, *Spectrochim. Acta A. Mol. Biomol. Spectrosc.* 71 (2009) 1901–1906.
- [55] F.V. Botelho, J.I. Alvarez-Leite, V.S. Lemos, A.M.C. Pimenta, H.D.R. Calado, T. Matencio, C.T. Miranda, E.C. Pereira-Maia, Physicochemical study of floranol, its copper(II) and iron(III) complexes, and their inhibitory effect on LDL oxidation, *J. Inorg. Biochem.* 101 (2007) 935–943.
- [56] Q. Wang, Z.Y. Yang, G.F. Qi, D.D. Qin, Synthesis, crystal structure, antioxidant activities and DNA-binding studies of the Ln(III) complexes with 7-methoxychromone-3-carbaldehyde-(4'-hydroxy) benzoyl hydrazone, *Eur. J. Med. Chem.* 44 (2009) 2425–2433.
- [57] T.R. Li, Z.Y. Yang, B.D. Wang, D.D. Qin, Synthesis, characterization, antioxidant activity and DNA-binding studies of two rare earth(III) complexes with naringenin-2-hydroxy benzoyl hydrazone ligand, *Eur. J. Med. Chem.* 43 (2008) 1688–1695.